Available online at www.sciencedirect.com
ScienceDirect
Journal of Sound and Vibration 309 (2008) 545–568
JOURNAL OF SOUND AND VIBRATION
www.elsevier.com/locate/jsvi

A hybrid formulation for mid-frequency analysis of assembled structures

A. Pratellesi[a,*], M. Viktorovitch[b], N. Baldanzini[a], M. Pierini[a]

[a]*DMTI—Dipartimento di Meccanica e Tecnologie Industriali, Universitá degli Studi di Firenze, Via di Santa Marta 3, 50139 Firenze, Italy*
[b]*Rieter Automotive AG, Center of Excellence—Vehicle Acoustics, Schlosstalstrasse 43, 8400 Winterthur, Switzerland*

Received 3 May 2006; received in revised form 19 July 2007; accepted 23 July 2007
Available online 10 September 2007

Abstract

A new formulation able to predict the behaviour of structures in the mid-frequency range is presented in this paper. The mid-frequency field is a hybrid domain for which assembled structures exhibit simultaneously low- and high-frequency behaviours, depending on the material and geometrical properties of different subsystems. Thus, dealing with the mid-frequency field requires simulation methods which are able to account the differences in behaviour of different subsystems. The hybrid formulation is based on the coupling of two different formulations, the finite elements for the low-frequency behaving subparts and a probabilistic formulation, the smooth integral formulation, applied to the high-frequency subsystems. The hybrid method enables to correctly predict the deterministic response of the low-frequency parts which is not affected by randomness, and the smooth trend of the contributions of the high-frequency parts. The paper is concluded with several numerical examples computed for coupled one- and two-dimensional structures.

1. Introduction

Being able to predict in the early design phases the vibro-acoustic behaviour of complex structures in the mid-frequency (MF) range, is nowadays a challenge of paramount importance in the industry. Among others, the transportation industry is particularly concerned since the notion of the vibro-acoustic comfort of the passenger is a crucial feature.

Generally, a complex mechanical structure can be defined as a system made of a large number of different components which exhibit large differences in terms of material and geometrical properties, and consequently have very different vibro-acoustic behaviour.

The automotive industry is used to divide the vibro-acoustics problematic in three separate domains, according to the frequency range. The low-frequency (LF) range is identified as the domain for which the dynamic behaviour of a complex structure can be expressed in terms of magnitude and phase of the response at discrete frequencies and locations. The dimensions of the subsystems may be considered short with respect

*Corresponding author. Tel.: +39 0554796287; fax: +39 0554796394.
E-mail address: alessandro.pratellesi@unifi.it (A. Pratellesi).
URL: http://www.pcm.unifi.it (A. Pratellesi).

0022-460X/$ - see front matter © 2007 Elsevier Ltd. All rights reserved.
doi:10.1016/j.jsv.2007.07.031

Nomenclature

$\mathbf{A}_{\mathrm{FEM}}$	FEM dynamic matrix
a_{ij}	ij element of FEM dynamic matrix
dG	first-order derivative of the Green kernel with respect to variable $\mathbf{x}$
E_i	Young modulus of subsystem i
$\mathbf{F}$	FEM vector of forces
f	external force
G	Green kernel function for the infinite system
$\mathbf{K}$	FEM stiffness matrix
k	stiffness value of FEM elements
$\mathbf{M}$	FEM mass matrix
m	mass value of FEM elements
N_T	number of boundary elements with first-order differentials boundary conditions
N_u	number of boundary elements with kinematic boundary conditions
S	section area
T_x	boundary force unknown at $\mathbf{x}$
u_x	boundary kinematic unknown at $\mathbf{x}$
w	rod longitudinal displacement
$\mathbf{x}$	vector of source point coordinates
$\mathbf{y}$	vector of external force coordinates
∂w_i	first-order derivative with respect to x of rod displacement, evaluated at point x_i
$\partial\Omega$	boundary of the domain
$\partial\Omega_T$	partition of $\partial\Omega$ with first-order differential boundary conditions
$\partial\Omega_u$	partition of $\partial\Omega$ with kinematic boundary conditions
$\boldsymbol{\xi}$	vector of field point coordinates
Ω	domain of analysis
Ω_f	partition of Ω with external forces applied
$\hat{}$	accent of boundary conditions
$\tilde{}$	accent of random variables

to the wavelength (short members). On the other hand, the high-frequency (HF) field is defined as the frequency range for which the components of a system are long with respect to the wavelength (long members). This characteristic implies that the presence of small uncertainties in the properties of the subsystems can dramatically influence the response of the structure. Finally, the MF domain is defined as a transition region. In this field, the structure is constituted of two classes of subsystems, respectively, exhibiting a LF and a HF behaviour.

Nowadays, different approaches are used for performing vibro-acoustic simulations, according to the frequency range and to the type of the structure. Deterministic element-based methods, like finite element method (FEM) [1] or boundary element method (BEM) [2,3], are successfully used to predict the dynamical response of a structure, and they are able to provide local and narrow-band solutions. The current computational resources allows these numerical methods to be efficient even for complex structures as far as the LF domain is concerned.

However, as the frequency increases, the wavelengths decrease and hence the discretization mesh of the structures must be refined. On the other hand, the increasing sensitivity of the responses to small perturbations implies that performing deterministic simulations is meaningless, and it is therefore much more relevant to develop formulations able to predict a priori the statistical vibrational response in terms of expectations and statistical moments.

The statistical energy analysis (SEA) is widely employed for solving HF problems [4–7]. SEA is a substructuring analysis method which is aimed at predicting the energy levels space and frequency averaged. SEA is generally used for structure-borne or air-borne excitations, even though the former set of applications might not be straightforward, depending on the complexity of the modelled structure (definition of junctions, power inputs, etc.). Employing relevantly the SEA requires to verify some hypotheses: the structure shall be non-zero damped, input powers shall be uncorrelated and the subsystems weakly coupled, the system shall present a reverberant field. Furthermore, the modal density of each subsystem shall be high; usually those requirements are not completely verified for realistic industrial structures.

The energy flow methods (EFM) are a different approach to the vibro-acoustical analysis in the HF range. They are derived from a local energy balance leading to a constitutive relationship analogous to the heat conduction equations. The numerical cost for solving the thermal problem is reduced compared to the wave-based approach. Many applications of these methods were proposed in the past [8–11]. However, the main

drawback of this approach concerns the validity of its theoretical background when dealing with two- and three-dimensional systems [12,13]. An alternative method for HF analysis have been proposed by Le Bot [14] which does not take into account interferences between propagative waves, it is asymptotic and hence more accurate as the frequency increases. The method is based on energetic quantities and energy balance but unlike SEA, which involves global variables, this method considers local variables.

For predicting the MF response, different approaches were proposed in the last decade, such as the so-called structural SEA [15], which aims at treating the structure-borne contribution of a car from a few hundred Hertz upward, by means of the SEA. For this purpose, the authors developed a methodology to define in a reliable way the subsystems of a structure without violating the basic assumptions of the SEA.

Le Bot recently proposed a hybrid approach for the MF range [16]. The noise radiated by a structure vibrating in the LF range is predicted using the so-called radiative transfer method. A modal description of the structure is coupled with an energy integral formulation for the acoustic cavity. In a first stage, the acceleration and the pressure fields on the surface of the vibrating structures are calculated. Then, the cross-spectra of these variables are used as inputs in the energy integral formulation. One major assumption of the method is that randomness is introduced to the phase of the acceleration and the surface pressure fields to account for the influence of inherent uncertainties in physical and geometrical properties. On the other hand, no randomness is introduced in the acoustic space description and thus, the Green's functions present in the formulation are similar to those usually employed in the classical integral representations.

Langley and Shorter developed a hybrid method [17–19] which couples FE and SEA formulations. The FE method is used to describe the components of a system that have a few modes (or a long free wavelength when compared to the dimensions), and that consequently exhibit a fairly robust dynamic behaviour. Alternatively, the SEA method is used to describe the uncertain components (with many modes or short wavelength). The result yielded by the method is the dynamic response averaged over an ensemble of uncertain structures. The global equations of motion include a contribution to the dynamic stiffness matrix and the forcing vector arising from the presence of the local response. The main effect of the local mode dynamics is to add damping and effective mass to the global modes, similar to the fuzzy structure theory.

The fuzzy structure theory was introduced by Soize in order to predict the response of a master structure coupled with a large number of secondary structures [20]. The attached subsystems are the so-called fuzzy substructures and are considered difficult to model by means of conventional methods due to the complexity in geometry and/or material properties. The primary objective of the fuzzy structure theory is to compute the response of the master structure while accounting for the influence of all the secondary structures. A random boundary impedance operator was introduced in order to describe the effects of mass and damping of fuzzy substructures on the master structure in the MF range. The solution is obtained using a recursive method or a Monte Carlo method.

In other respects, Vlahopoulos et al. [21–23] developed a hybrid FEA approach which combines conventional FEA with EFEA to achieve a numerical solution for systems comprised by stiff and flexible members. Stiff and flexible members are modelled by conventional FEA and EFEA, respectively. It is assumed that a complex structure is divided into "long" components that have relatively HF vibration, and "short" components that have relatively LF vibration. The key challenge was in capturing the energy transfer at junctions between long and short components. They handled this by relating the displacement and slope in the conventional finite element (FE) formulation to the amplitude of the impinging wave in the energy FE formulation for each junction between long and short components. This so-called hybrid joint leads to the EFEA power transfer coefficients at long–short junctions that complement the power transfer coefficients at long–long junctions. The latter are calculated analytically by modelling a long component as a semi-infinite structure. The solution process was then to calculate the response of the long members first, and then calculate the response of the short members, subject to incoherent excitation at the short–long joints, using conventional FEA.

This paper is concerned with the MF problematic and aims at presenting an alternative formulation able to predict the behaviour of a complex structure in this frequency domain.

The starting point is a formulation priorly developed by Viktorovitch et al. [24,25] so-called the Smooth Integral Formulation (SIF). It is based on a boundary integral formulation coupled with a statistical approach to account for uncertainties in the structural parameters [26]. The underlying idea is that a structure always

encounters physical uncertainties which play an increasing role when the frequency increases. According to Fahy [27], the differences among systems which share the same design characteristics, and the effects of these differences on vibrational behaviour are individually unpredictable in the HF, therefore a probabilistic model is appropriate. Thus, introducing randomness to the geometrical or/and material properties of the structure leads to a precise description of the deterministic LF response and a smooth response in the HF field corresponding to the "average" of the strongly oscillating vibratory response. In between, a transition zone is observed in which the response gradually shifts from the deterministic to the average response. In order to solve the problem, some fundamental assumptions dealing with the correlation among the unknowns of the formulation are introduced. Those assumptions allows to obtain a close system solution of the SIF which does not requires a recursive method.

The stochastic characterization of the boundaries allows to give a consistent vibro-acoustic description of structures on the whole frequency range.

The hybrid formulation described in this article aims at coupling the SIF employed for the HF part of the structure, with the FE description of the LF behaving subsystems. The coupling allows to account for both deterministic and statistical contributions in the response of the structure, and therefore to obtain a consistent formulation for the MF range.

This paper is organized as follows: in Section 2, the fundamental relationships of the SIF are derived. In Section 3 a HF application of the SIF is presented. Section 4 defines the MF problematic and how the SIF can be applied to this domain. The hybrid FEM–SIF method is finally derived in Section 5, and numerically applied in Section 6.

2. High-frequency modelling thanks to the Smooth Integral Formulation

In the HF field, the vibrational response of a structure is dramatically sensitive to small perturbations of its geometrical and material properties. Thus, solving the usual constitutive equations describing the vibrational behaviour of the structure, by means of a usual numerical solver is generally meaningless. To overcome this problem, randomness is introduced to the description of the geometry of the structure and a formulation exhibiting explicitly the expectations of the usual kinematic unknowns, with respect to the randomness, is derived. This randomness should not affect the response in the LF field, on the other hand, the aim is to obtain a smooth response in the HF field highlighting the overall trend of the fast varying deterministic behaviour.

In other respect, writing a first-order moment formulation is useless since these variables vanish to zero when the frequency rises. Therefore, the formulation must be written on the second-order unknowns.

The constitutive equations of the SIF derived in previous papers [24,25] are reminded in what follows.

2.1. The random formulation for isolated structures

The initial stage for deriving the SIF equations is a direct boundary integral formulation. The formulation is very general and stands for one-, two- and three-dimensional problems. The integral representation for a homogeneous, isotropic and linear mechanical system of domain Ω and smooth boundary $\partial\Omega$, subjected to a harmonic loading f, may be written

$$c \cdot u(\boldsymbol{\xi}) = \int_{\Omega_f} f(\mathbf{y}) \cdot G(\mathbf{y}, \boldsymbol{\xi}) \, \mathrm{d}\Omega + \int_{\partial\Omega} (u(\mathbf{x}) \cdot dG(\mathbf{x}, \boldsymbol{\xi}) - T(\mathbf{x}) \cdot G(\mathbf{x}, \boldsymbol{\xi})) \, \mathrm{d}\partial\Omega. \tag{1}$$

The integral representation is completed with the following boundary conditions:

$$\begin{cases} u(\mathbf{x}) = \hat{u}(\mathbf{x}) & \text{on } \partial\Omega_u \\ T(\mathbf{x}) = \hat{T}(\mathbf{x}) & \text{on } \partial\Omega_T \end{cases} \quad \text{and} \quad \begin{cases} c = \frac{1}{2}, & \boldsymbol{\xi} \in \partial\Omega, \\ c = 0 & \text{otherwise}, \end{cases}$$

where $u(\mathbf{x})$ is the kinematic unknown (e.g. pressure, displacement), T is the boundary force unknown, G denotes the Green kernel, dG is the first-order derivative of the Green kernel with respect to the variable $\mathbf{x}$, $\partial\Omega_u$ and $\partial\Omega_T$ constitute a partition of $\partial\Omega$.

A randomness is then applied to the locations of the loading and the boundary of the structure. These two new random parameters are, respectively, denoted by $\tilde{\Omega}_f$ and $\partial\tilde{\Omega}$. Accordingly, the partition of the boundary becomes $\partial\tilde{\Omega} = \partial\tilde{\Omega}_T \cup \partial\tilde{\Omega}_u$.

N_u and N_T are, respectively, the number of boundary elements defined for $\partial\tilde{\Omega}_u$ and $\partial\tilde{\Omega}_T$. The collocation method is employed which enables the transformation of the integral equations, Eq. (1), into a discrete set of equations. As an illustration, the equation evaluated at point $\tilde{\boldsymbol{\xi}} \in \partial\tilde{\Omega}_u$ is reported. $\tilde{u}_j$ is the boundary random unknown at element j.

$$\frac{1}{2}u_\xi = \int_{\tilde{\Omega}_f} f(\mathbf{y}) \cdot G(\mathbf{y}, \tilde{\boldsymbol{\xi}})\,\mathrm{d}\Omega + \sum_{j=1}^{N_T} \int_{\partial\tilde{\Omega}_j} [u_j \cdot dG(\mathbf{x}, \tilde{\boldsymbol{\xi}}) - \hat{T}_j \cdot G(\mathbf{x}, \tilde{\boldsymbol{\xi}})]\,\mathrm{d}\partial\Omega + \sum_{k=1}^{N_u} \int_{\partial\tilde{\Omega}_k} [\hat{u}_k \cdot dG(\mathbf{x}, \tilde{\boldsymbol{\xi}}) - T_k \cdot G(\mathbf{x}, \tilde{\boldsymbol{\xi}})]\,\mathrm{d}\partial\Omega. \tag{2}$$

The goal of this work is to derive an integral representation whose unknowns are the expectations of the cross-products of the force and displacement unknowns. Therefore, for any boundary location $\tilde{\boldsymbol{\xi}} \in \partial\tilde{\Omega}$, the right- and left-hand sides of Eq. (2) are multiplied by the conjugate of the random boundary unknown at the same spatial position. The expectations of the equations are finally considered. They are represented by $\langle - \rangle$.

Finally, $N_u + N_T$ boundary element equations are obtained.

2.2. Limiting the unknowns and final formulation

To solve the $N_u + N_T$ equations some statistical assumptions for limiting the number of unknowns are defined. These assumptions govern the correlation of the different variables appearing in the equations above. They are based on a physical interpretation of the integral equations in terms of source contributions. They were detailed in the previously mentioned publications [24,25].

The first assumption deals with the statistical behaviour of the different sources.

Assumption 1. The contributions of two sources are statistically independent when the positions of the sources or the target points of the contributions are distinct.

At this stage, two types of sources are distinguished; the external loadings which are called primary sources and the boundary sources (on which no loading is applied) which are called secondary sources. The latter are constituted by the multiple wave reflections of the waves stemming from the loadings.

The second assumption governs the random behaviour of the force and displacement variables.

Assumption 2. It is considered that a force or a displacement variable expressed at any point of the structure, is only correlated with the contributions of the primary sources at that point.

As an illustration, if we consider the term related to the contribution of the external force at point $\tilde{\mathbf{x}}_i$, $\langle \tilde{u}_i^* \cdot \int_{\tilde{\Omega}_f} f(\mathbf{y}) \cdot G(\mathbf{y}, \tilde{\mathbf{x}}_i)\,\mathrm{d}\Omega \rangle$ it cannot be split because f is a primary source for $\tilde{\mathbf{x}}_i$. Instead if we consider the contribution at $\tilde{\mathbf{x}}_i$ of source located at $\tilde{\mathbf{x}}_j$,

$$\left\langle \tilde{u}_i^* \cdot \sum_{\substack{j=1 \\ j \neq i}}^{N_T} \tilde{u}_j \int_{\partial\tilde{\Omega}_j} dG(\mathbf{x}, \tilde{\mathbf{x}}_i)\,\mathrm{d}\partial\Omega \right\rangle$$

according to Assumptions 1–2 this can be split as follows:

$$\langle \tilde{u}_i^* \rangle \cdot \sum_{\substack{j=1 \\ j \neq i}}^{N_T} \langle \tilde{u}_j \rangle \left\langle \int_{\partial\tilde{\Omega}_j} dG(\mathbf{x}, \tilde{\mathbf{x}}_i)\,\mathrm{d}\partial\Omega \right\rangle.$$

For assembled systems, we should classify the sources in a different way:

Assumption 3. The boundaries connecting two substructures, of which one contains a primary source, become primary sources for the other substructure.

This assumption expresses the correlation between an external loading and a force–displacement variable located on two different subsystems.

The development of the SIF formulation for a single rod structure is reported in Appendix A, together with an application to two coupled semi-infinite rods to illustrate the importance of the assumptions.

2.3. The fundamental equations of the SIF

Finally, applying the first two assumptions, the fundamental equations of the formulation may be written

- $\tilde{\mathbf{x}}_i \in \partial\tilde{\Omega}_i,\ i \in [1, N_T]$:

$$\begin{aligned}\frac{1}{2}\langle|\tilde{u}_i|^2\rangle = &\left\langle \tilde{u}_i^* \cdot \int_{\tilde{\Omega}_f} f(\mathbf{y}) \cdot G(\mathbf{y}, \tilde{\mathbf{x}}_i)\,\mathrm{d}\Omega \right\rangle + \langle \tilde{u}_i^* \rangle \cdot \sum_{\substack{j=1 \\ j\neq i}}^{N_T} \langle \tilde{u}_j \rangle \left\langle \int_{\partial\tilde{\Omega}_j} dG(\mathbf{x}, \tilde{\mathbf{x}}_i)\,\mathrm{d}\partial\Omega \right\rangle \\ &- \langle \tilde{u}_i^* \rangle \cdot \sum_{j=1}^{N_T} \left\langle \int_{\partial\tilde{\Omega}_j} \hat{T}_j \cdot G(\mathbf{x}, \tilde{\mathbf{x}}_i)\,\mathrm{d}\partial\Omega \right\rangle + \langle \tilde{u}_i^* \rangle \cdot \sum_{k=1}^{N_u} \left\langle \int_{\partial\tilde{\Omega}_k} \hat{u}_k \cdot dG(\mathbf{x}, \tilde{\mathbf{x}}_i)\,\mathrm{d}\partial\Omega \right\rangle \\ &- \langle \tilde{u}_i^* \rangle \cdot \sum_{k=1}^{N_u} \langle \tilde{T}_k \rangle \left\langle \int_{\partial\tilde{\Omega}_k} G(\mathbf{x}, \tilde{\mathbf{x}}_i)\,\mathrm{d}\partial\Omega \right\rangle + \langle|\tilde{u}_i|^2\rangle \cdot \left\langle \int_{\partial\tilde{\Omega}_i} dG(\mathbf{x}, \tilde{\mathbf{x}}_i)\,\mathrm{d}\partial\Omega \right\rangle. \end{aligned} \tag{3}$$

- $\tilde{\mathbf{x}}_i \in \partial\tilde{\Omega}_i,\ i \in [1, N_u]$:

$$\begin{aligned}\frac{1}{2}\langle \tilde{T}_i^* \rangle \cdot \hat{u}_i = &\left\langle \tilde{T}_i^* \cdot \int_{\tilde{\Omega}_f} f(\mathbf{y}) \cdot G(\mathbf{y}, \tilde{\mathbf{x}}_i)\,\mathrm{d}\Omega \right\rangle + \langle \tilde{T}_i^* \rangle \cdot \sum_{j=1}^{N_T} \langle \tilde{u}_j \rangle \left\langle \int_{\partial\tilde{\Omega}_j} dG(\mathbf{x}, \tilde{\mathbf{x}}_i)\,\mathrm{d}\partial\Omega \right\rangle \\ &- \langle \tilde{T}_i^* \rangle \cdot \sum_{j=1}^{N_T} \left\langle \int_{\partial\tilde{\Omega}_j} \hat{T}_j \cdot G(\mathbf{x}, \tilde{\mathbf{x}}_i)\,\mathrm{d}\partial\Omega \right\rangle + \langle \tilde{T}_i^* \rangle \cdot \sum_{k=1}^{N_u} \left\langle \int_{\partial\tilde{\Omega}_k} \hat{u}(\mathbf{x}) \cdot dG(\mathbf{x}, \tilde{\mathbf{x}}_i)\,\mathrm{d}\partial\Omega \right\rangle \\ &- \langle \tilde{T}_i^* \rangle \cdot \sum_{\substack{k=1 \\ k\neq i}}^{N_u} \langle \tilde{T}_k \rangle \left\langle \int_{\partial\tilde{\Omega}_k} G(\mathbf{x}, \tilde{\mathbf{x}}_i)\,\mathrm{d}\partial\Omega \right\rangle - \langle|\tilde{T}_i|^2\rangle \cdot \left\langle \int_{\partial\tilde{\Omega}_i} G(\mathbf{x}, \tilde{\mathbf{x}}_i)\,\mathrm{d}\partial\Omega \right\rangle. \end{aligned} \tag{4}$$

Eqs. (3) and (4) are the fundamental relationships of the SIF. The number of unknowns in these equations is equal to $3(N_u + N_T)$. These unknowns are:

- First-order moments: $\langle \tilde{u}_i \rangle$ and $\langle \tilde{T}_i \rangle$.
- Second-order moments: $\langle|\tilde{u}_i|^2\rangle$ and $\langle|\tilde{T}_i|^2\rangle$.
- Expectation of the kinematic variables multiplied by the contribution of the primary source: $\langle \tilde{u}_i^* \cdot \int_{\tilde{\Omega}_f} f(\mathbf{y}) \cdot G(\mathbf{y}, \tilde{\mathbf{x}}_i)\,\mathrm{d}\Omega \rangle$ and $\langle \tilde{T}_i^* \cdot \int_{\tilde{\Omega}_f} f(\mathbf{y}) \cdot G(\mathbf{y}, \tilde{\mathbf{x}}_i)\,\mathrm{d}\Omega \rangle$.

In order to obtain a consistent set of equations, $2(N_u + N_T)$ supplementary equations are added to the formulation [24,25]. $(N_u + N_T)$ equations are the expectation of the standard integral equation evaluated in $\tilde{\boldsymbol{\xi}} = \tilde{\mathbf{x}}_i \in \partial\tilde{\Omega}_i,\ i = 1, \ldots, N_u + N_T$. The remaining equations are generated from the integral equation multiplied by the conjugate of the contribution of the external force $\int_{\tilde{\Omega}_f} f^*(\mathbf{y}) \cdot G^*(\mathbf{y}, \tilde{\mathbf{x}}_i)\,\mathrm{d}\Omega$, evaluated in $\tilde{\boldsymbol{\xi}} = \tilde{\mathbf{x}}_i \in \partial\tilde{\Omega}_i,\ i = 1, 2, \ldots, N_u + N_T$.

2.4. Application of the random formulation

The SIF was applied to various one- and two-dimensional structures and the numerical results were reported in previous publications [24,25]. As an example, the SIF is applied in this paper to two coupled rods with one rod subjected to a longitudinal external excitation, Fig. 1. The geometries of the structures are

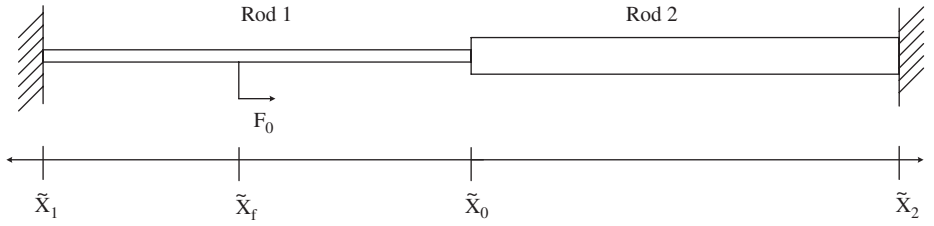

Fig. 1. Structure made of two coupled rods. Clamped–clamped boundary conditions.

Table 1
SIF numerical application

	Length (m)	x_f (m)	E (N/m^2)	S (m^2)	η (%)	ρ (kg/m^3)
Rod 1	3.64	1.96	2.1×10^{11}	10^{-4}	2	7800
Rod 2	8.83		2.1×10^{09}	10^{-5}	0.2	7800

Parameters of the coupled rod system.

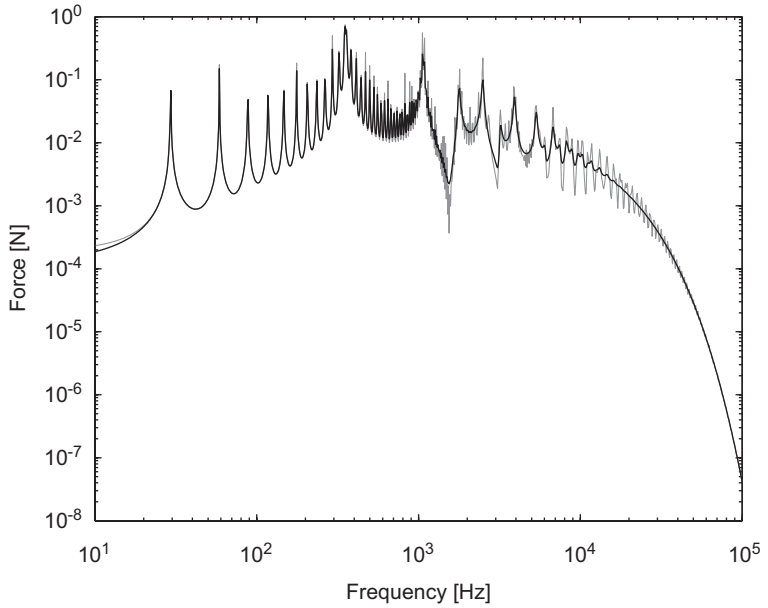

Fig. 2. Frequency evolution of the modulus of the traction at x_2 for the structure made of two coupled rods, $\sigma = 0.04$: ———SIF; ———BEM.

perturbed by Gaussian random variables defined by their mean value and standard deviation. The mechanical and geometrical properties of the structure are given in Table 1.

The traction at the boundary x_2 of rod 2 is depicted in Fig. 2. Comparing the responses obtained with the SIF with the deterministic results, leads to the following analysis:

(1) The influence of the randomness increases with frequency.
(2) The SIF is able to represent precisely the frequency response in the LF domain.
(3) The HF part of the SIF prediction is smooth and only delivers information on the general trend of the frequency variation of the boundary unknowns.

3. Simplifying the SIF equations for applications in the high-frequency field

The SIF, which is very general, is able to cover the full frequency range, the response in the LF domain being analogous to a deterministic computation, whereas in the HFs the introduction of randomness gives a frequency average-like response.

However, applying this formulation in the LF field is useless due to a higher number of unknowns when compared for instance to a classical BEM formulation.

When restricting the use of the SIF to the HF domain, the number of unknowns can be reduced. It can be observed that the expectations of the kinematic variables converge quickly to zero when the frequency increases, Fig. 3. It is therefore not necessary to calculate these variables, which may be a priori set to zero when HF simulations are performed. As an example, when considering isolated systems it can be deduced from Section 2.3, that getting rid of the first-order moments leads to writing a set of equations containing $2(N_u + N_T)$ unknowns instead of $3(N_U + N_T)$. The simplified SIF was verified for two assembled rods (Fig. 1). The frequency variation of the square traction at the coupling point between the two rods is depicted in Fig. 4. The geometrical and material properties of the rods are summarized in Table 2. As expected, the SIF response is smooth and actually gives the correct trend of the response in the HF field. On the other hand, not taking into account the first-order moments leads to removing the modal peaks which are predicted by the "full" SIF in the LF field. The results of the SIF are compared to those obtained with the BEM applied to the deterministic structure.

4. Modifying the SIF equations for mid-frequency field applications

When dealing specifically with the MF field (defined in the introduction of the paper as the frequency domain for which a structure can be divided into two parts, one presenting a LF behaviour and the other a HF behaviour) some simplifications of the general formulation of the SIF can be performed. These are performed taking into consideration that:

(1) The first-order moments of the random subsystems are neglected.
(2) It is useless to randomly describe the LF behaving subsystems, their response being not affected by the randomness.

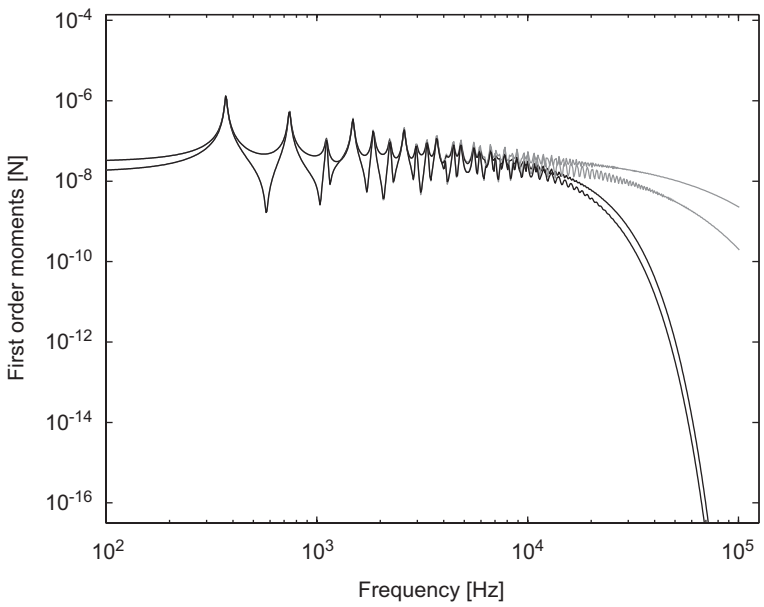

Fig. 3. Frequency evolution of the first-order moments, traction, at x_1 and x_2 single rod structure, $\sigma = 0.05$: ———Expectation values; ———Deterministic values.

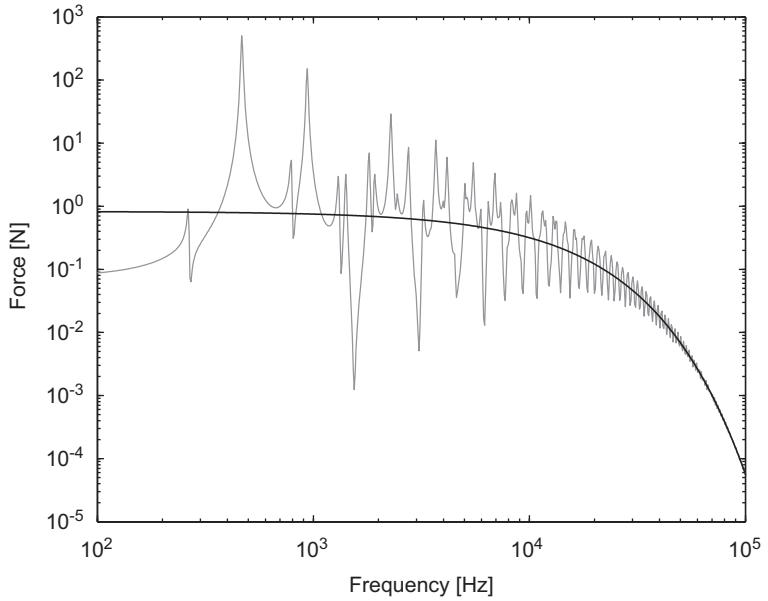

Fig. 4. Frequency evolution of the traction at x_0 for the structure made of two coupled rods, $\sigma = 0.02$: ———high-frequency SIF; ———BEM.

Table 2
High-frequency SIF numerical application

	Length (m)	x_f (m)	E (N/m^2)	S (m^2)	η (%)	ρ (kg/m^3)
Rod 1	5.64	3.96	2.1×10^{11}	10^{-5}	2	7800
Rod 2	4.83		2.1×10^{11}	10^{-4}	2	7800

Parameters of the coupled rod system.

Despite the deterministic description of the LF subsystems, the variables calculated for these substructures should be considered random. The fact of introducing randomness on a specific subsystem influences the response of the overall structure.

4.1. Derivation of the SIF fundamental equations in the mid-frequency field

In this section, the equations of the SIF are derived for a simple structure made of two coupled rods with a longitudinal loading (Fig. 1). The SIF equations for this example can be obtained from the procedure reported in Section 2. As a simplification of the formulation, scalar variables will replace the vector description.

It is assumed that due to its specific geometrical and material properties, rod 1 should not be randomized. As an illustration, the integral equations dealing with the first-order moments of rod 1, are reported. The notations are simplified by writing $\partial w(x_i)$ instead of $\partial w(x_i)/\partial x$:

$$0 = \langle \partial w(x_1) \rangle G_1(x_1, x_1) - \langle \partial w(x_0) \rangle G_1(x_1, x_0) + \langle w(x_0) \rangle dG_1(x_1, x_0), \tag{5}$$

$$0 = \langle \partial w(x_1) \rangle G_1(x_0, x_1) - \langle \partial w(x_0) \rangle G_1(x_0, x_0) + \langle w(x_0) \rangle (dG_1(x_0, x_0) - 1). \tag{6}$$

In these equations, the Green kernels are deterministic, due to the fact that the spatial points for which the fundamental solutions are evaluated are deterministic.

In other respect, combining Eqs. (5) and (6), one can prove that the boundary unknowns expressed at points x_0 and x_1 are correlated:

$$\langle \partial w(x_1)\rangle = -\langle \partial w(x_0)\rangle \frac{\dfrac{dG_1(x_1,x_0)}{G_1(x_1,x_0)} - \dfrac{dG_1(x_0,x_0)-1}{G_1(x_0,x_0)}}{\dfrac{G_1(x_1,x_1)}{G_1(x_1,x_0)} - \dfrac{G_1(x_1,x_1)}{G_1(x_1,x_0)}}. \tag{7}$$

Eq. (7) shows that the two boundary unknowns expressed at x_0 and x_1 are linked via a deterministic coefficient. Therefore, supplementary second-order moments, appear in the equations, such as $\langle \partial w^*(x_1)\cdot \partial w(x_0)\rangle$.

Finally, one can write the following equations for rod 1:

$$0 = \langle |\partial w(x_1)|^2\rangle G_1(x_1,x_1) - \langle \partial w(x_0)\cdot \partial w^*(x_1)\rangle G_1(x_1,x_0) + \langle w(x_0)\cdot \partial w^*(x_1)\rangle dG_1(x_1,x_0), \tag{8}$$

$$0 = \langle \partial w(x_1)\cdot \partial w^*(x_0)\rangle G_1(x_0,x_1) - \langle |\partial w(x_0)|^2\rangle G_1(x_0,x_0) + \langle w(x_0)\cdot \partial w^*(x_0)\rangle (dG_1(x_0-x_0)-1), \tag{9}$$

$$0 = \langle \partial w(x_1)\cdot w^*(x_0)\rangle G_1(x_0,x_1) - \langle \partial w(x_0)\cdot w^*(x_0)\rangle G_1(x_0,x_0) + \langle |w(x_0)|^2\rangle (dG_1(x_0,x_0)-1). \tag{10}$$

The complete set equations for the MF application of the SIF to a structure made of two subsystems, is detailed in Appendix B.

4.2. Numerical application of the reformulated SIF for mid-frequency simulations

In this section, the hybrid formulation is applied to two coupled rods, Fig. 5 with geometrical and material properties summarized in Table 3. Rod 1 is stiff and short and thus modelled deterministically, Eqs. (8)–(10), while rod 2 is flexible and long and is treated as random. The loading is applied on the HF rod (rod 2). The randomness is introduced to the boundary x_2 of rod 2 and at the force location.

The frequency variations of the second-order moments—traction of the boundary of rod 2 and displacement at the junction between the two rods—are depicted in Figs. 6 and 7. Below 10^4 Hz (for this specific example), the quick oscillations are represented by a smooth curve representing the overall deterministic response. Simultaneously, the peaks corresponding to the modes of the LF subsystem are precisely described.

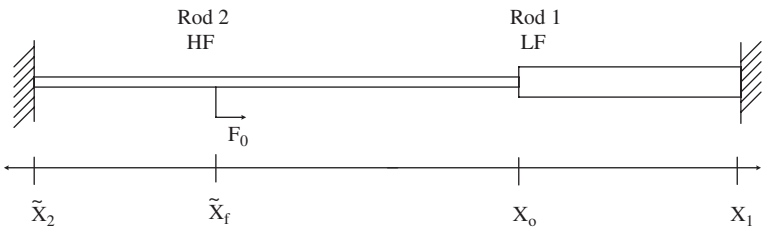

Fig. 5. Structure made of two coupled rods. Clamped–clamped boundary conditions. Rod 1 deterministic, Rod 2 random.

Table 3
Mid-frequency SIF numerical application

	Length (m)	x_f (m)	E (N/m^2)	S (m^2)	η (%)	ρ (kg/m^3)
Rod 1	1.13		2.1×10^{11}	10^{-3}	2	7800
Rod 2	8.64	4.96	2.1×10^{10}	10^{-5}	0.2	7800

Parameters of the coupled rod system.

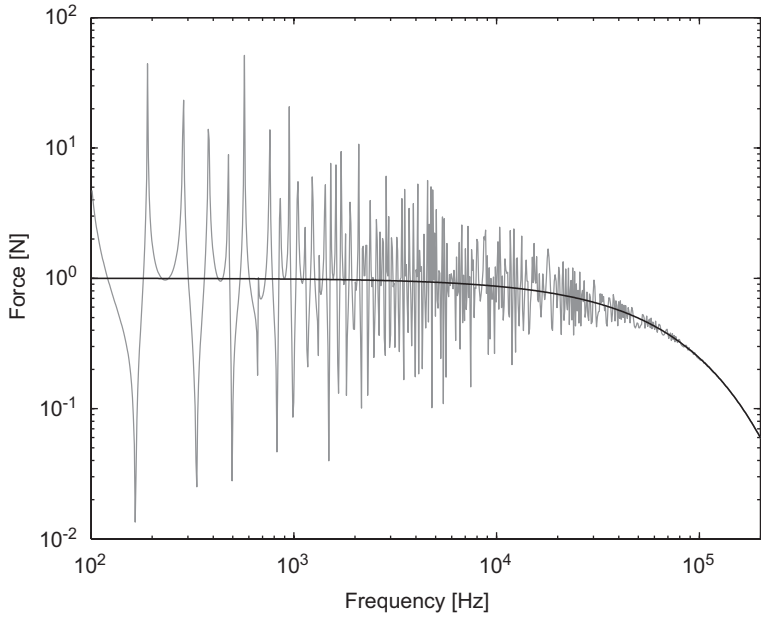

Fig. 6. Mid-frequency application of SIF. Frequency evolution of the modulus of traction at x_2 for the structure made of two coupled rods, $\sigma = 0.05$: ———mid-frequency SIF; ———BEM.

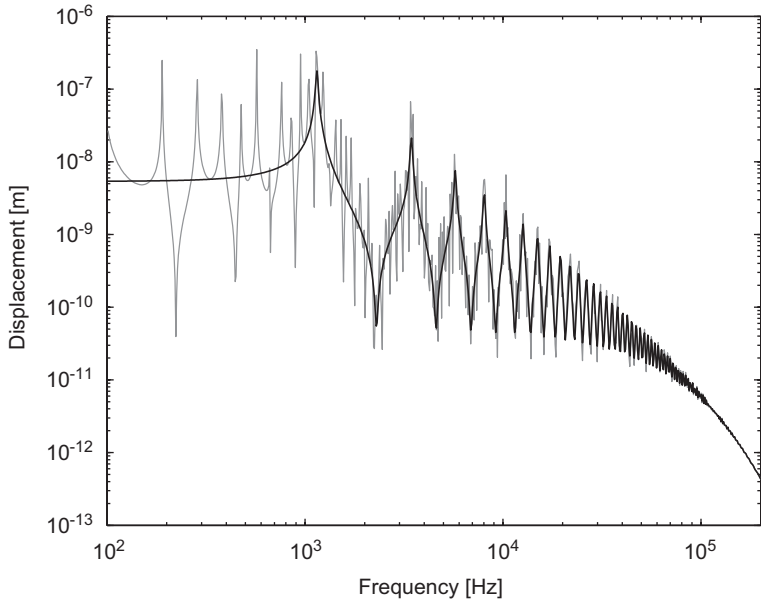

Fig. 7. Mid-frequency application of SIF. Frequency evolution of the modulus of displacement at x_0 for the structure made of two coupled rods, $\sigma = 0.05$: ———mid-frequency SIF; ———BEM.

When the first-order moments are included in the formulation, the complete SIF is able to predict the first eigenfrequencies of the HF subsystems (rod 2 in this case), while the SIF formulation with no first-order moments, produces a smooth contribution of the HF subsystem in the whole frequency range. Therefore, the modified SIF expressed without first-order moments, is representative of the structure behaviour in the MF range, but not in the LF range (Fig. 8).

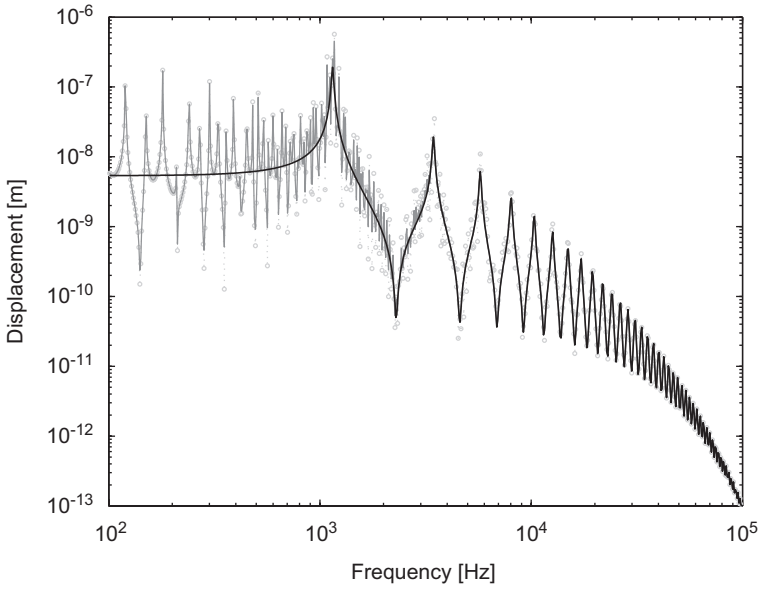

Fig. 8. Confrontation of different formulation of SIF theory and deterministic results. Frequency evolution of the modulus of displacement at x_0, $\sigma = 0.05$: ———mid-frequency SIF; ———SIF; -○ -○ -BEM.

5. A new approach for mid-frequency modelling: coupling FEM and SIF

The aim of this section is to derive a hybrid MF formulation coupling the SIF and the FEM. The LF behaving subsystems are modelled with the FEM while the HF behaving subsystems are modelled with the SIF. Contrary to some current hybrid formulations coupling SEA and FE, this method does not present the theoretical difficulty to couple force–displacement variables with energy quantities.

In this section, the formulation is explicitly derived for a one-dimensional structure made of two subsystems. It can be extended to any kind of two- and three-dimensional structures.

The external loading is applied to the random HF behaving subsystem and the first-order moments are suppressed from the formulation, assuming that these unknowns rapidly vanish to zero.

Considering the deterministic substructure, submitted to a harmonic external excitation, it is possible to obtain the general FEM formulation, as follows:

$$\mathbf{A}_{\mathrm{FEM}} \cdot \mathbf{u}_{\mathrm{FEM}} = \mathbf{F} \quad \text{and} \quad \mathbf{A}_{\mathrm{FEM}} = [\mathbf{K} - \omega^2 \cdot \mathbf{M}], \tag{11}$$

$\mathbf{u}_{\mathrm{FEM}}$ is the nodal vector of unknowns, $\mathbf{A}_{\mathrm{FEM}}$ is the dynamic matrix, and $\mathbf{F}$ denotes the nodal external forces. The external excitations on the boundaries of the deterministic subsystem can be expressed as functions of the boundary unknowns. For instance, considering a clamped boundary element, at the clamped node j, one has

$$w_j = 0, \quad ES \cdot \frac{\partial w_j}{\partial x} = F_j, \tag{12}$$

where F_j is the external force applied by the clamp to the element j, and x is the direction of longitudinal displacement.

For each node of the FE model, one can write the equilibrium equations at each node (Fig. 9):

$$a_{ii-1} \cdot u_{i-1} + a_{ii} \cdot u_i + a_{ii+1} \cdot u_{i+1} = F_i \tag{13}$$

and

$$a_{ii} = k_{ii} - \omega^2 \cdot m_{ii},$$

where k_{ii} is the concentrated stiffness at node i, while m_{ii} represents the concentrated mass.

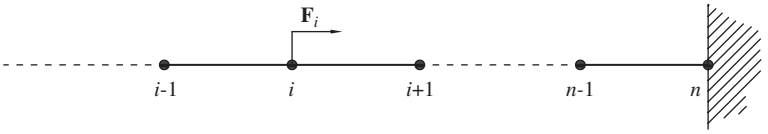

Fig. 9. FEM elements scheme.

The aim is now to rewrite Eq. (11) in order to obtain a FE formulation which can be coupled to the SIF description.

As explained in the previous section, the first-order moments vanish to zero in the MF and HF range, for all the subsystems. Among other reasons, this is due to the fact that the unknowns of the LF behaving subsystems are random even if the subsystem is geometrically deterministic. This randomness is due to the HF subsystems which are geometrically randomized.

The unknowns of the SIF formulation are the second-order moments of the kinematic boundary unknowns. Therefore, to couple the SIF model with the FE description, one needs to adapt the FE description to make it consistent with the SIF formulation. A procedure analogous to the one introduced in Section 2.3, is used. For each node, the corresponding equilibrium equation (Eq. (13)) is multiplied by the conjugate of the nodal unknown at the same spatial position. n second-order equations are finally obtained:

$$a_{ii-1} \cdot \langle u_{i-1} \cdot u_i^* \rangle + a_{ii} \cdot \langle |u_i|^2 \rangle + a_{ii+1} \cdot \langle u_{i+1} \cdot u_i^* \rangle = F_i \cdot \langle u_i^* \rangle. \tag{14}$$

The FEM subsystem is deterministically described, therefore according to Section 4.1, decorrelation between the nodal variables may not be assumed. Hence, the full set of unknowns present in Eq. (14) shall be solved. Supplementary equations are added to obtain a number of equations equal to the number of unknowns. These equations are obtained by multiplying the nodal equations, Eq. (13) by the conjugate of the unknowns, respectively, expressed at nodes i and $i-1$:

$$a_{ii-1} \cdot \langle |u_{i-1}|^2 \rangle + a_{ii} \cdot \langle u_i \cdot u_{i-1}^* \rangle + a_{ii+1} \cdot \langle u_{i+1} \cdot u_{i-1}^* \rangle = F_i \cdot \langle u_{i-1}^* \rangle \tag{15}$$

and

$$a_{ii-1} \cdot \langle u_{i-1} \cdot u_{i+1}^* \rangle + a_{ii} \cdot \langle u_i \cdot u_{i+1}^* \rangle + a_{ii+1} \cdot \langle |u_{i+1}|^2 \rangle = F_i \cdot \langle u_{i+1}^* \rangle. \tag{16}$$

A linear system with $5n$ unknowns must be solved. To the $3n$ equations (Eqs. (14)–(16)), $2n$ supplementary equations are generated, considering the conjugates of Eqs. (15) and (16).

Finally, Eqs. (14)–(16) can be written into a matrix form:

$$\mathbf{B}_{\mathrm{FEM}} \cdot \langle \mathbf{u}_{\mathrm{FEM}}^2 \rangle = 0, \tag{17}$$

where $\mathbf{B}_{\mathrm{FEM}}$ is the matrix of coefficient, and $\mathbf{u}_{\mathrm{FEM}}^2$ is the vector of the second-order unknowns containing both square modules $\langle |u_i|^2 \rangle$ and cross-product terms $\langle u_i^* \cdot u_j \rangle$.

To solve more effectively the numerical system, a condensation technique is introduced. This technique enabled the authors to reduce the overall number of unknowns of the formulation. One obtains

$$\mathbf{B}_{\mathrm{FEM}} = \left[\begin{array}{c|c} \mathbf{B}_{bb} & \mathbf{B}_{bi} \\ \hline \mathbf{B}_{ib} & \mathbf{B}_{ii} \end{array}\right] \text{ and } \left[\begin{array}{c|c} \mathbf{B}_{bb} & \mathbf{B}_{bi} \\ \hline \mathbf{B}_{ib} & \mathbf{B}_{ii} \end{array}\right] \cdot \left\{\begin{array}{c} \langle \mathbf{u}_{\mathrm{FEM}}^2 \rangle_{\mathrm{boundaries}} \\ \langle \mathbf{u}_{\mathrm{FEM}}^2 \rangle_{\mathrm{internal}} \end{array}\right\} = 0 \tag{18}$$

Evaluating $\langle \mathbf{u}_{\mathrm{FEM}}^2 \rangle_{\mathrm{internal}}$ from the lower part of Eq. (18) and substituting in the upper part:

$$\begin{cases} \langle \mathbf{u}_{\mathrm{FEM}}^2 \rangle_{\mathrm{internal}} = \mathbf{B}_{ii}^{-1} \cdot \mathbf{B}_{ib} \cdot \langle \mathbf{u}_{\mathrm{FEM}}^2 \rangle_{\mathrm{boundaries}}, \\ \{\mathbf{B}_{bb} - \mathbf{B}_{bi} \cdot \mathbf{B}_{ii}^{-1} \cdot \mathbf{B}_{ib}\} \cdot \langle \mathbf{u}_{\mathrm{FEM}}^2 \rangle_{\mathrm{boundaries}} = 0, \end{cases}$$

$$\mathbf{B}_{\mathrm{reduced}} = \{\mathbf{B}_{bb} - \mathbf{B}_{bi} \cdot \mathbf{B}_{ii}^{-1} \cdot \mathbf{B}_{ib}\}$$

and

$$\mathbf{B}_{\text{reduced}} \cdot \langle \mathbf{u}^2_{\text{FEM}} \rangle_{\text{boundaries}} = 0. \tag{19}$$

$\mathbf{B}_{\text{reduced}}$ is the matrix obtained after applying the reduction technique.

The developments above highlight that even though the unknowns that must be solved are not the usual first-order kinematic variable, the element of the matrices involved in the relationships, are the usual components of the original FE formulation. Once the reduced matrix has been calculated, the second-order system can be solved.

At last, Eqs. (19) for the FEM, and the SIF relationships without the first-order moments, are considered for the hybrid formulation. The force–displacement coupling relationships are added to obtain a consistent set of equations.

6. Numerical application of the FEM-SIF theory

Two different numerical applications are reported in this section, to assess the validity and the effectiveness of the hybrid formulation. The entire formulation will be developed for the structure made of two coupled rods.

6.1. The case of two coupled rods

The formulation defined above is applied to two coupled rods (Fig. 10), with geometrical and material properties summarized in Table 4. Rod 1 is stiff and short and thus modelled deterministically, while rod 2 is flexible and long and is considered random. The structure is clamped at its boundary points. The loading is applied on the HF rod. The randomness is introduced to the boundaries of rod 2 and to the force location. The FE subsystem (rod 1) is subjected to an external excitation located at the nodes 0 and n (corresponding to the geometrical locations x_0 and x_1). The loading can be expressed as

$$F_0 = E_1 S_1 \cdot \partial w_0, \quad F_n = E_1 S_1 \cdot \partial w_n.$$

The $n+1$ FE basic equilibrium equations expressed for each node of rod 1 may be written:

$$\begin{cases} a_{00} \cdot w_0 + a_{01} \cdot w_1 = E_1 S_1 \cdot \partial w_0, \\ a_{10} \cdot w_0 + a_{11} \cdot w_1 + a_{12} \cdot w_2 = 0, \\ \vdots \\ a_{n-1n-2} \cdot w_{n-2} + a_{n-1n-1} \cdot w_{n-1} + a_{n-1n} \cdot w_n = 0, \\ a_{nn-1} \cdot w_{n-1} + a_{nn} \cdot w_n = E_1 S_1 \cdot \partial w_n. \end{cases} \tag{20}$$

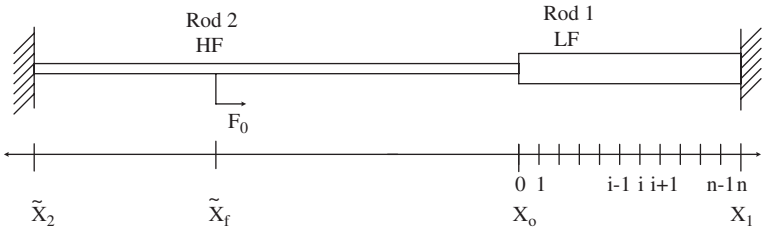

Fig. 10. Structure made of two coupled rods. Clamped–clamped boundary conditions. FEM discretization of the deterministic rod.

Table 4
FEM–SIF numerical application

	Length (m)	x_f (m)	E (N/m^2)	S (m^2)	η (%)	ρ (kg/m^3)
Rod 1	1.13		2.1×10^{11}	10^{-3}	2	7800
Rod 2	8.64	4.96	2.1×10^{10}	10^{-5}	0.2	7800

Parameters of the coupled rod system.

The FE Eqs. (20), are multiplied by the conjugate of the relevant nodal unknowns and the expectations of the different equations are considered.

Finally, at node i, one can write

$$a_{ii-1} \cdot \langle w_{i-1} \cdot w_i^* \rangle + a_{ii} \cdot \langle |w_i|^2 \rangle + a_{ii+1} \cdot \langle w_{i+1} \cdot w_i^* \rangle = 0, \tag{21}$$

$$a_{ii-1} \cdot \langle |w_{i-1}|^2 \rangle + a_{ii} \cdot \langle w_i \cdot w_{i-1}^* \rangle + a_{ii+1} \cdot \langle w_{i+1} \cdot w_{i-1}^* \rangle = 0, \tag{22}$$

$$a_{ii-1} \cdot \langle w_{i-1} \cdot w_{i+1}^* \rangle + a_{ii} \cdot \langle w_i \cdot w_{i+1}^* \rangle + a_{ii+1} \cdot \langle |w_{i+1}|^2 \rangle = 0 \tag{23}$$

and the corresponding unknowns related to node i:

$$\langle |w_i|^2 \rangle, \langle w_{i-1} \cdot w_i^* \rangle \langle w_{i+1} \cdot w_i^* \rangle, \langle w_{i-1} \cdot w_{i+1}^* \rangle, \langle w_{i-1}^* \cdot w_{i+1} \rangle.$$

The HF behaving rod is modelled with the SIF. Five equations may be written and eight unknowns are generated:

- Expectation of square modulus of boundary unknowns

$$\langle |\partial w(x_0)|^2 \rangle, \langle |w(x_0)|^2 \rangle, \langle |\partial w(\tilde{x}_2)|^2 \rangle.$$

- Expectations of cross-product of unknowns at coupling point

$$\langle w(x_0) \cdot \partial w^*(x_0) \rangle, \langle |w^*(x_0) \cdot \partial w(x_0)|^2 \rangle.$$

- Expectations of boundary unknowns multiplied by the contribution of the external force:

$$\langle \partial w^*(x_0) G_2(x_0, \tilde{x}_f) \rangle, \langle w^*(x_0) G_2(x_0, \tilde{x}_f) \rangle, \langle \partial w^*(x_2) G_2(x_2, \tilde{x}_f) \rangle.$$

Four coupling equations, written at the coupling point x_0 shall be as well expressed: the continuity of displacement (written in terms of square displacement modulus), of the traction, the product of displacement with the conjugate of the traction and the conjugate of the latter product.

Evaluating the number of equations and unknowns shows that $2n$ more equations are required, which can be obtained considering the conjugate of the second-order FEM equations, Eqs. (21)–(23). The consistent set of equations for the entire structure is constituted of $5n + 10$ equations. The condensation technique explicated previously is now applied to the second-order linear system of equations of the subsystem modelled with FEM. The dimension of the deterministic matrix, $\mathbf{B}_{\mathrm{FEM}}$, is reduced from $[(5n + 1) \times (5n + 2)]$ to $[4 \times 5]$. The modelling of rod 1 is finally condensed to five unknowns:

$$\langle \mathbf{u}_{\mathrm{FEM}}^2 \rangle_{\mathrm{boundaries}} = \begin{bmatrix} \langle |w_0|^2 \rangle \\ \langle w_0 \cdot \partial w_0^* \rangle \\ \langle w_0^* \cdot \partial w_0 \rangle \\ \langle |\partial w_0|^2 \rangle \\ \langle |\partial w_n|^2 \rangle \end{bmatrix}$$

and four equations:

$$\mathbf{B}(1,1)_{\mathrm{reduced}} \cdot \langle |w_0|^2 \rangle + \mathbf{B}(1,2)_{\mathrm{reduced}} \cdot \langle w_0 \cdot \partial w_0^* \rangle + \mathbf{B}(1,3)_{\mathrm{reduced}} \cdot \langle w_0^* \cdot \partial w_0 \rangle + \mathbf{B}(1,5)_{\mathrm{reduced}} \cdot \langle |\partial w_n|^2 \rangle = 0, \tag{24}$$

$$\mathbf{B}(2,1)_{\mathrm{reduced}} \cdot \langle |w_0|^2 \rangle + \mathbf{B}(2,2)_{\mathrm{reduced}} \cdot \langle w_0 \cdot \partial w_0^* \rangle + \mathbf{B}(2,3)_{\mathrm{reduced}} \cdot \langle w_0^* \cdot \partial w_0 \rangle + \mathbf{B}(2,4)_{\mathrm{reduced}} \cdot \langle |\partial w_0|^2 \rangle = 0, \tag{25}$$

$$\mathbf{B}(3,1)_{\mathrm{reduced}} \cdot \langle |w_0|^2 \rangle + \mathbf{B}(3,2)_{\mathrm{reduced}} \cdot \langle w_0 \cdot \partial w_0^* \rangle + \mathbf{B}(3,3)_{\mathrm{reduced}} \cdot \langle w_0^* \cdot \partial w_0 \rangle = 0, \tag{26}$$

$$\mathbf{B}(4,1)_{\mathrm{reduced}} \cdot \langle |w_0|^2 \rangle + \mathbf{B}(4,2)_{\mathrm{reduced}} \cdot \langle w_0 \cdot \partial w_0^* \rangle + \mathbf{B}(4,3)_{\mathrm{reduced}} \cdot \langle w_0^* \cdot \partial w_0 \rangle = 0. \tag{27}$$

Finally, using the four equations above, five equations for rod 2 and four coupling relations, one obtains a consistent linear [13 × 13] system.

The frequency variations of the second-order moments, the traction at the boundary of rod 1 and the displacement at the junction between the two rods, are illustrated in Figs. 11 and 12. Like in Section 4.2, a smooth response is obtained for the unknowns of the random rod, and a detailed description of the response of the deterministic rod. The upper value of the frequency range has been limited to 20 000 Hz even if this formulation produces exact results above this frequency limit. The reason is that when frequency increases, rod 1 finally reaches the domain where its contribution to the global response of the structure can be identified as a HF contribution. Thus, the global structure has moved from the MF domain to the HF field. Figs. 11 and 12 illustrate that coupling FEM and SIF theory to model a MF behaving structure leads to relevant results.

6.2. Numerical application for a two-dimensional-acoustical domain

The hybrid formulation has been used to predict the response of a structure made of two coupled two-dimensional-acoustical domains (Fig. 13). Domain 1 exhibits a HF behaviour in the frequency range of interest. Randomness is introduced to its boundaries and to the force location. Domain 2 is LF behaving and is deterministically described. The coupling boundary between domain 1 and 2 is deterministic. The physical properties of the structure, which have been defined to satisfy the MF condition, are reported in Table 5. The external excitation is located at point $x_f = 0.41m$, $y_f = 0.23m$. Domain 1 is modelled with the SIF, and randomness ($\sigma = 0.05$) is introduced to the boundaries which are not coupled with domain 2 (deterministic and modelled with FEM). In this example, the first-order moments are kept in the formulation in order to correctly describe the behaviour of the structure in the LF field.

The frequency variations of the pressure at two distinct locations, on domains 1 and 2, respectively, are depicted in Figs. 14 and 15. The frequency variation of the response is gradually getting smoother when the frequency increases for the domain 1, and simultaneously, an accurate description of the response of the deterministic domain is obtained.

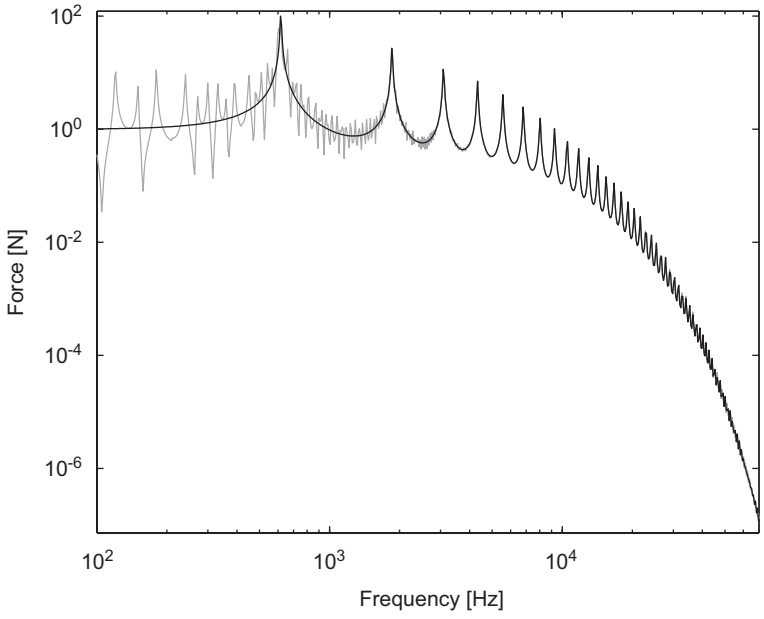

Fig. 11. Application of hybrid FEM–SIF formulation. Frequency evolution of the modulus of traction at x_1 for the structure made of two coupled rods: ———FEM–SIF; – – –BEM.

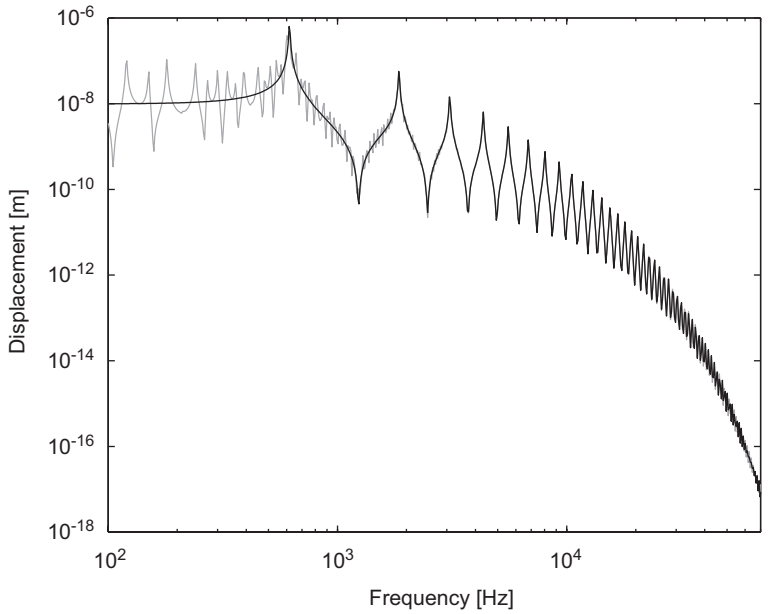

Fig. 12. Application of hybrid FEM–SIF formulation. Frequency evolution of the modulus of displacement at x_0 for the structure made of two coupled rods: ———FEM–SIF; ———BEM.

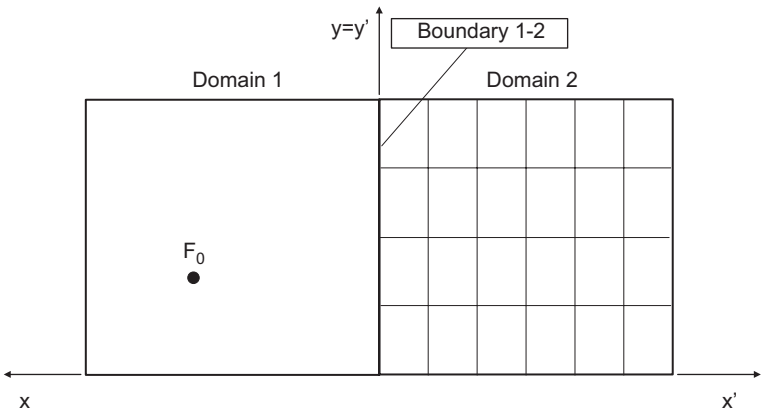

Fig. 13. Structure made of two coupled acoustical domain.

Table 5
FEM–SIF numerical application

	Side length (m)	Sound speed (m/s)	ρ (kg/m^2)	η (%)
Domain 1	1.0	25	10	0.02
Domain 2	1.0	600	250	0.02

Parameters of the coupled acoustical domains.

6.3. Discussion

In Table 6, the information regarding the computation parameters for the acoustic domains described in Section 6.2 is reported. The number of elements and the computational times for the hybrid calculation and a

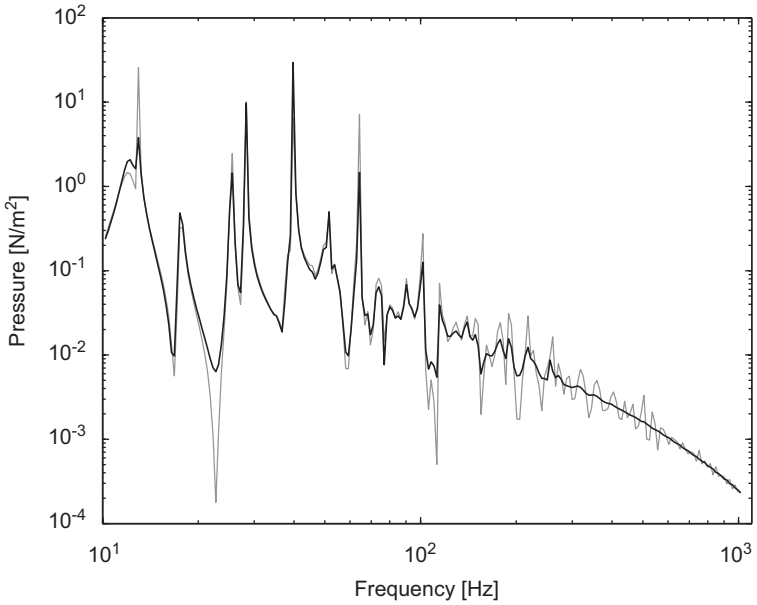

Fig. 14. Application of hybrid FEM–SIF formulation. Frequency evolution of the pressure value at a boundary node of domain 1: ———FEM–SIF; ———FEM–BEM.

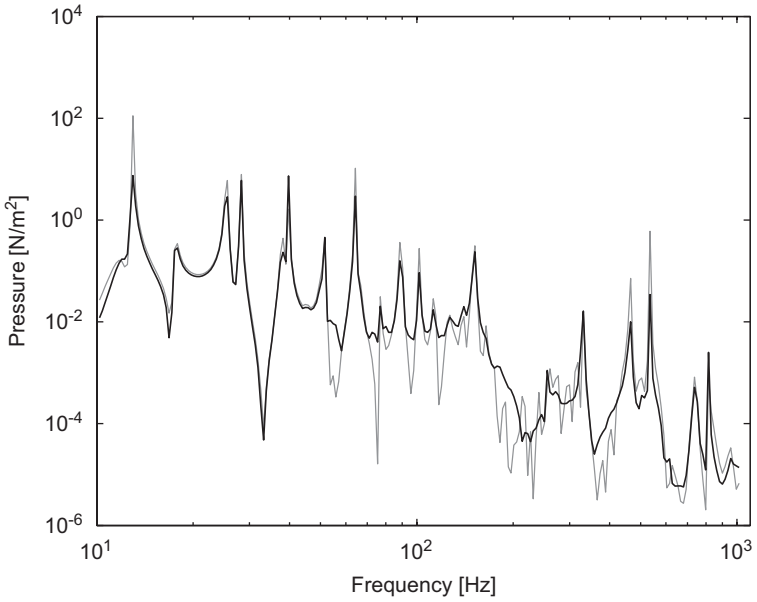

Fig. 15. Application of hybrid FEM–SIF formulation. Frequency evolution of the pressure value of an internal node of domain 2: ———FEM–SIF; ———FEM–BEM.

usual FE–BEM solution are compared. First, it is shown that the number of elements required for performing a relevant calculation with the FEM–SIF was dramatically reduced. In the MF field, the subsystems modelled with FE (and hence LF behaving) do not require a refined discretization because their dimensions are short with respect to the wavelength. As already discussed in previous sections, the subsystems modelled with SIF do not need as well, a refined discretization, due to the slow spatial variations of the responses. Furthermore, a

Table 6
Computational details, single-frequency confrontation

	FEM–BEM	FEM–SIF
Number of elements	8420	480
Computational time (s)	2850	460

computational time comparison between FE–SIF and FEM–BEM is reported in Table 6. As expected, the computational resources required for the FEM–SIF calculation are much lower than those for the FEM–BEM. The computing time differences are directly related with the number of elements used to describe the structure for both formulations.

In other respect, the frequency step that is used for the calculations may be sensitively coarsen when employing the FEM–SIF formulation. The "non-modal" output obtained for the HF subsystems, which leads to a smooth frequency response enables to link the frequency step to the wavelength of the LF subsystems, which are characterized by a low modal density. This allows us to reduce the number of frequency calculation steps for the hybrid method, and thus sensitively reduce the calculation times.

7. Conclusion

In this paper, the fundamentals of the SIF were summarized. A numerical application of the SIF was proposed for a two coupled rods structure, in order to illustrate the effectiveness of this approach on a wide frequency range. It was shown that in the low frequencies the SIF is able to precisely describe the successive modes and when the frequency increases the SIF prediction is able to give the trend of the strongly oscillating deterministic response. The SIF was then applied to the HF domain. In this domain, the number of unknowns can be reduced, because it is not necessary to calculate the first-order moments, which converge to zero. This enables to decrease the number of unknowns. The HF SIF response is smooth and effectively gives the correct trend of the response.

Then, a hybrid formulation coupling the SIF with a FE formulation was derived for MF applications. For this purpose, it was assumed that:

- the MF range is the domain within which a structure is constituted of two parts, a stiff part exhibiting a LF behaviour, and a flexible part with a HF behaviour;
- the properties of a structure are intrinsically uncertain. This global uncertainty plays no role in the LF field, on the other hand it has a large influence on the HF responses.

The entire formulation was derived for a structure made of two subsystems, the LF part are modelled with FE whereas the flexible part is modelled with SIF. This novel formulation was applied to two different structures, two coupled rods and a two-dimensional system made of two coupled acoustical domains. The results show that the hybrid formulation is able to accurately catch the modal behaviour of the LF subsystems and give the smooth trend of the fast varying response, contribution of the HF subsystems.

Appendix A. SIF formulation and assumptions

The aim of this appendix is to highlight each step of the SIF formulation in a comprehensive way. For this purpose, the SIF equations are derived for a simple one-dimensional structure, an isolated rod. The unknowns and the set of equations of the SIF are defined and the utilization of the two first statistical assumptions (introduced in Section 2.2) is highlighted.

In a second stage, the SIF equations are derived for a structure made of two coupled semi-infinite rods, in order to explain the role of the third assumption (defined in Section 2.2).

A.1. Deriving the SIF equations for a clamped rod

The boundary integral equations for a clamped/clamped rod (Fig. 16) subjected to a point loading F_0 may be written

$$w(x_1) = \frac{F_0}{ES} \cdot G(x_1, x_f) + \partial w(x_2) \cdot G(x_1, x_2) - \partial w(x_1) \cdot G(x_1, x_1), \tag{A.1}$$

$$w(x_2) = \frac{F_0}{ES} \cdot G(x_2, x_f) + \partial w(x_2) \cdot G(x_2, x_2) - \partial w(x_1) \cdot G(x_2, x_1). \tag{A.2}$$

The geometrical parameters encountered in Eqs. (A.1) and (A.2) are x_1, x_2 and x_f, corresponding to the respective positions of the boundaries and the location of the loading. These parameters, when randomly defined may be expressed as follows:

$$\tilde{x}_1 = x_1 + \varepsilon_1, \quad \tilde{x}_2 = x_2 + \varepsilon_2, \quad \tilde{x}_f = x_f + \varepsilon_f,$$

where ε_1, ε_2 and ε_f denote independent zero mean random variables. Despite the positions of the boundaries are randomly defined, the boundary conditions are deterministic and therefore, one can write in the case of a clamped rod: $w(\tilde{x}_1) = w(\tilde{x}_2) = 0$. Using the random notations, Eqs. (A.1) and (A.2), become:

$$0 = \frac{F_0}{ES} \cdot G(\tilde{x}_1, \tilde{x}_f) + \partial w(\tilde{x}_2) \cdot G(\tilde{x}_1, \tilde{x}_2) - \partial w(\tilde{x}_1) \cdot G(\tilde{x}_1, \tilde{x}_1), \tag{A.3}$$

$$0 = \frac{F_0}{ES} \cdot G(\tilde{x}_2, \tilde{x}_f) + \partial w(\tilde{x}_2) \cdot G(\tilde{x}_2, \tilde{x}_2) - \partial w(\tilde{x}_1) \cdot G(\tilde{x}_2, \tilde{x}_1). \tag{A.4}$$

The SIF relationships are obtained by multiplying each side of Eq. (A.3) (respectively, Eq. (A.4)), by the conjugate of the unknown boundary kinematic variable, $\partial w^*(\tilde{x}_1)$ (respectively, $\partial w^*(\tilde{x}_2)$). The expectations with respect to $\tilde{x}_1$, $\tilde{x}_2$ and $\tilde{x}_f$ (represented by the symbol $\langle - \rangle$) of the two sides of the equations are then taken into account, one obtains from Eq. (A.3):

$$0 = \frac{F_0}{ES} \cdot \langle \partial w^*(\tilde{x}_1) \cdot G(\tilde{x}_1, \tilde{x}_f) \rangle + \langle \partial w^*(\tilde{x}_1) \cdot \partial w(\tilde{x}_2) \cdot G(\tilde{x}_1, \tilde{x}_2) \rangle - \langle |\partial w(\tilde{x}_1)|^2 \rangle \cdot G(\tilde{x}_1, \tilde{x}_1). \tag{A.5}$$

A similar relationship is obtained from Eq. (A.4).

Employing the statistical assumptions one and two introduced in Section 2.2, which define the correlations between the variables present in Eq. (A.5), the term $\langle \partial w^*(\tilde{x}_1) \cdot \partial w(\tilde{x}_2) \cdot G(\tilde{x}_1, \tilde{x}_2) \rangle$ may be modified as follows:

From Assumption 1, stating that a boundary unknown and the contribution of a secondary source located on a boundary are decorrelated, one can write

$$\langle \partial w^*(\tilde{x}_1) \cdot \partial w(\tilde{x}_2) \cdot G(\tilde{x}_1, \tilde{x}_2) \rangle = \langle \partial w^*(\tilde{x}_1) \rangle \cdot \langle \partial w(\tilde{x}_2) \cdot G(\tilde{x}_1, \tilde{x}_2) \rangle.$$

From Assumption 2, defining that the amplitude of a source and the Green kernel defined between two distinct points are decorrelated, one can finally write

$$\langle \partial w^*(\tilde{x}_1) \cdot \partial w(\tilde{x}_2) \cdot G(\tilde{x}_1, \tilde{x}_2) \rangle = \langle \partial w^*(\tilde{x}_1) \rangle \cdot \langle \partial w(\tilde{x}_2) \rangle \cdot \langle G(\tilde{x}_1, \tilde{x}_2) \rangle.$$

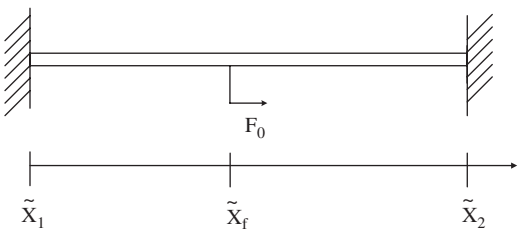

Fig. 16. Single rod structure with random boundaries. Clamped–clamped boundary conditions.

Using the two statistical assumptions, Eq. (A.5) may finally be written

$$0 = \frac{F_0}{ES} \cdot \langle \partial w^*(\tilde{x}_1) \cdot G(\tilde{x}_1, \tilde{x}_f) \rangle + \langle \partial w^*(\tilde{x}_1) \rangle \cdot \langle \partial w(\tilde{x}_2) \rangle \cdot \langle G(\tilde{x}_1, \tilde{x}_2) \rangle - \langle |\partial w(\tilde{x}_1)|^2 \rangle \cdot G(\tilde{x}_1, \tilde{x}_1). \tag{A.6}$$

The same procedure is used to derive the SIF equation at the boundary $\tilde{x}_2$. The SIF formulation for an isolated rod generates:

- Four second-order unknowns: $\langle |w(\tilde{x}_1)|^2 \rangle$, $\langle |w(\tilde{x}_2)|^2 \rangle$, $\langle \partial w^*(\tilde{x}_1) \cdot G(\tilde{x}_1, \tilde{x}_f) \rangle$, $\langle \partial w^*(\tilde{x}_2) \cdot G(\tilde{x}_2, \tilde{x}_f) \rangle$.
- Two first-order unknowns $\langle w(\tilde{x}_1) \rangle$, $\langle w(\tilde{x}_2) \rangle$.

Thus, in addition to two equations (A.5), four supplementary equations are required in order to estimate the six unknowns. Two equations are obtained by considering the expectation of the first-order integral equations (A.3) and (A.4). Two more equations are obtained by multiplying each side of the conjugate of Eq. (A.3) (respectively, Eq. (A.4)) by $\cdot G(\tilde{x}_1, \tilde{x}_f)$ (respectively, $\cdot G(\tilde{x}_2, \tilde{x}_f)$). One obtains

$$0 = \left(\frac{F_0}{ES}\right)^* \cdot \langle |G(\tilde{x}_1, \tilde{x}_f)|^2 \rangle + \langle \partial w^*(\tilde{x}_2) \rangle \cdot \langle G^*(\tilde{x}_1, \tilde{x}_2) \rangle \cdot \langle G(\tilde{x}_1, \tilde{x}_f) \rangle - \langle \partial w^*(\tilde{x}_1) \cdot G(\tilde{x}_1, \tilde{x}_f) \rangle \cdot G^*(\tilde{x}_1, \tilde{x}_1). \tag{A.7}$$

It can be observed that the variables in the term $\langle \partial w^*(\tilde{x}_1) \cdot G(\tilde{x}_1, \tilde{x}_f) \rangle$ are assumed correlated, due to the fact that $F_0/ES \cdot G(\tilde{x}_1, \tilde{x}_f)$ is the contribution in x_1 of a primary source. According to Assumption 1, this variable is correlated with the boundary unknown $\partial w(\tilde{x}_1)$.

A.2. Deriving the SIF equations for two assembled rods

A structure made of two co-linear coupled semi-infinite rods is analysed (Fig. 17) in order to highlight the role of the third assumption. For this purpose, the SIF equation are written at a location $\tilde{x}$ distinct from the coupling position. It is therefore assumed that the boundary SIF equations were previously solved. The random boundary equation at $\tilde{x}$ is

$$w(\tilde{x}) = \partial w(\tilde{x}_0) \cdot G(\tilde{x}, \tilde{x}_0) - w(\tilde{x}_0) \cdot dG(\tilde{x}, \tilde{x}_0), \tag{A.8}$$

where $\tilde{x}_0$ denotes the randomized boundary location. The SIF formulation is obtained by multiplying each side of Eq. (A.8), by the conjugate of $w(\tilde{x})$:

$$\langle |w(\tilde{x})|^2 \rangle = \langle w^*(\tilde{x}) \cdot \partial w(\tilde{x}_0) \cdot G(\tilde{x}, \tilde{x}_0) \rangle - \langle w^*(\tilde{x}) \cdot w(\tilde{x}_0) \cdot dG(\tilde{x}, \tilde{x}_0) \rangle. \tag{A.9}$$

The terms present in Eq. (A.9) such as

$$\langle w^*(\tilde{x}) \cdot \partial w(\tilde{x}_0) \cdot G(\tilde{x}, \tilde{x}_0) \rangle, \quad \langle w^*(\tilde{x}) \cdot w(\tilde{x}_0) \cdot dG(\tilde{x}, \tilde{x}_0) \rangle$$

are made of variables which cannot be considered as uncorrelated. Indeed, according to assumption three, the boundary point $\tilde{x}_0$, is a primary source for rod 2. Hence its contribution, $w(\tilde{x}_0) \cdot dG(\tilde{x}, \tilde{x}_0)$ is correlated with the displacement at $\tilde{x}$. The presence of these unknowns, requires to introduce two more equations in order to solve Eq. (A.9). The additional equations are generated by multiplying the conjugate of Eq. (A.8) by

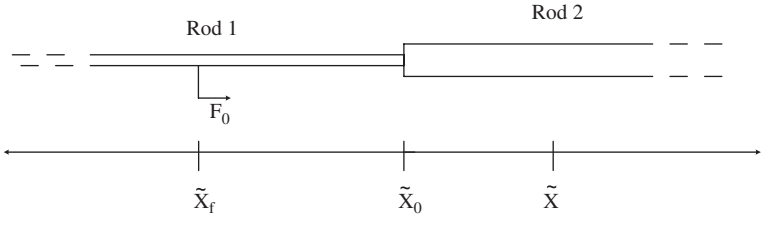

Fig. 17. Structure made of two coupled semi-infinite rods with random boundaries.

$\partial w(\tilde{x}_0)\cdot G(\tilde{x},\tilde{x}_0)$ and $w(\tilde{x}_0)\cdot dG(\tilde{x},\tilde{x}_0)$, respectively. One finally obtains the following supplementary equations:

$$\langle w^*(\tilde{x})\cdot\partial w(\tilde{x}_0)\cdot G(\tilde{x},\tilde{x}_0)\rangle = \langle|\partial w^*(\tilde{x}_0)|^2\rangle\cdot\langle|G(\tilde{x},\tilde{x}_0)|^2\rangle - \langle w^*(\tilde{x}_0)\cdot\partial w(\tilde{x}_0)\rangle\cdot\langle G(\tilde{x},\tilde{x}_0)\cdot dG^*(\tilde{x},\tilde{x}_0)\rangle, \tag{A.10}$$

$$\langle w^*(\tilde{x})\cdot w(\tilde{x}_0)\cdot dG(\tilde{x},\tilde{x}_0)\rangle = \langle\partial w^*(\tilde{x}_0)\cdot w(\tilde{x}_0)\rangle\cdot\langle dG(\tilde{x},\tilde{x}_0)\cdot G^*(\tilde{x},\tilde{x}_0)\rangle - \langle|w(\tilde{x}_0)|^2\rangle\cdot\langle|dG(\tilde{x},\tilde{x}_0)|^2\rangle. \tag{A.11}$$

Appendix B. SIF formulation for mid-frequency applications

B.1. Random subsystem

The first-order moments are neglected.

- The fundamental equation of SIF formulation for MF application to a random-subsystem.
  - $\tilde{\mathbf{x}}_i \in \partial\tilde{\Omega}_i$, $i \in [1, N_T]$:

$$\frac{1}{2}\langle|\tilde{u}_i|^2\rangle = \left\langle \tilde{u}_i^* \cdot \int_{\tilde{\Omega}_f} f(\mathbf{y})\cdot G(\mathbf{y},\tilde{\mathbf{x}}_i)\,\mathrm{d}\Omega \right\rangle + \langle|\tilde{u}_i|^2\rangle\left\langle \int_{\partial\tilde{\Omega}_i} dG(\mathbf{x},\tilde{\mathbf{x}}_i)\,\mathrm{d}\partial\Omega \right\rangle. \tag{B.1}$$

  - $\tilde{\mathbf{x}}_i \in \partial\tilde{\Omega}_i$, $i \in [1, N_u]$:

$$0 = \left\langle \tilde{T}_i^* \int_{\tilde{\Omega}_f} f(\mathbf{y})G(\mathbf{y},\tilde{\mathbf{x}}_i)\,\mathrm{d}\Omega \right\rangle - \langle|\tilde{T}_i|^2\rangle\left\langle \int_{\partial\tilde{\Omega}_i} G(\mathbf{x},\tilde{\mathbf{x}}_i)\,\mathrm{d}\partial\Omega \right\rangle. \tag{B.2}$$

- Auxiliary equations of SIF formulation for MF application to a random-subsystem.

For $\tilde{\mathbf{x}}_i \in \partial\tilde{\Omega}_i$, $i = 1, 2, \ldots, N_u + N_T$:

$$\begin{aligned}\frac{1}{2}\left\langle \tilde{u}_i)\int_{\tilde{\Omega}_f} f^*(\mathbf{y})\cdot G^*(\mathbf{y},\tilde{\mathbf{x}}_i)\,\mathrm{d}\Omega \right\rangle = {} & \left\langle \left| \int_{\tilde{\Omega}_f} f(\mathbf{y})\cdot G(\mathbf{y},\tilde{\mathbf{x}}_i)\,\mathrm{d}\Omega \right|^2 \right\rangle \\ & - \sum_{j=1}^{N_T}\left\langle \int_{\tilde{\Omega}_f} f^*(\mathbf{y})\cdot G^*(\mathbf{y},\tilde{\mathbf{x}}_i)\,\mathrm{d}\Omega \right\rangle\left\langle \int_{\partial\tilde{\Omega}_j} \hat{T}_j\cdot G(\mathbf{x},\tilde{\mathbf{x}}_i)\,\mathrm{d}\partial\Omega \right\rangle \\ & + \sum_{k=1}^{N_u}\left\langle \int_{\tilde{\Omega}_f} f^*(\mathbf{y})\cdot G^*(\mathbf{y},\tilde{\mathbf{x}}_i)\,\mathrm{d}\Omega \right\rangle\left\langle \int_{\partial\tilde{\Omega}_k} \hat{u}_k\cdot dG(\mathbf{x},\tilde{\mathbf{x}}_i)\,\mathrm{d}\partial\Omega \right\rangle \\ & + c_j\cdot\left\langle \tilde{u}_i\cdot\int_{\tilde{\Omega}_f} f^*(\mathbf{y})\cdot G^*(\mathbf{y},\tilde{\mathbf{x}}_i)\,\mathrm{d}\Omega \right\rangle\left\langle \int_{\partial\tilde{\Omega}_j} dG(\mathbf{x},\tilde{\mathbf{x}}_i)\,\mathrm{d}\partial\Omega \right\rangle \\ & - c_k\cdot\left\langle \tilde{T}_i\cdot\int_{\tilde{\Omega}_f} f^*(\mathbf{y})\cdot G^*(\mathbf{y},\tilde{\mathbf{x}}_i)\ \mathrm{d}\Omega \right\rangle\left\langle \int_{\partial\tilde{\Omega}_k} G(\mathbf{x},\tilde{\mathbf{x}}_i)\,\mathrm{d}\partial\Omega \right\rangle\end{aligned} \tag{B.3}$$

with

$$\begin{cases} c_j = 0 & \forall\tilde{\mathbf{x}}_i \in \partial\tilde{\Omega}_u \\ c_j = 1 & \forall\tilde{\mathbf{x}}_i \in \partial\tilde{\Omega}_T \end{cases} \quad \text{and} \quad \begin{cases} c_k = 0 & \forall\tilde{\mathbf{x}}_i \in \partial\tilde{\Omega}_T, \\ c_k = 1 & \forall\tilde{\mathbf{x}}_i \in \partial\tilde{\Omega}_u. \end{cases}$$

B.2. Deterministic subsystem

- The fundamental equation of SIF formulation for MF application to a deterministic-subsystem.
  - $\mathbf{x}_i \in \partial\Omega_i,\ i \in [1, N_T]$:

$$\frac{1}{2}\langle|u_i|^2\rangle = \sum_{\substack{j=1\\ j\neq i}}^{N_T}\langle u_i^* \cdot u_j\rangle \int_{\partial\Omega_j} dG(\mathbf{x},\mathbf{x}_i)\,\mathrm{d}\partial\Omega - \sum_{k=1}^{N_u}\langle u_i^* \cdot T_k\rangle \int_{\partial\Omega_k} G(\mathbf{x},\mathbf{x}_i)\,\mathrm{d}\partial\Omega + \langle|u_i|^2\rangle \int_{\partial\Omega_i} dG(\mathbf{x},\mathbf{x}_i)\,\mathrm{d}\partial\Omega, \tag{B.4}$$

  - $\mathbf{x}_i \in \partial\Omega_i,\ i \in [1, N_u]$:

$$0 = \sum_{j=1}^{N_T}\langle T_i^* \cdot u_j\rangle \int_{\partial\Omega_j} dG(\mathbf{x},\mathbf{x}_i)\,\mathrm{d}\partial\Omega - \sum_{\substack{k=1\\ k\neq i}}^{N_u}\langle T_i^* \cdot T_k\rangle \int_{\partial\Omega_k} G(\mathbf{x},\mathbf{x}_i)\,\mathrm{d}\partial\Omega - \langle|T_i|^2\rangle \int_{\partial\Omega_i} G(\mathbf{x},\mathbf{x}_i)\,\mathrm{d}\partial\Omega. \tag{B.5}$$

References

[1] O.C. Zienkiewicz, R.L. Taylor, *The Finite Element Method*, Butterworth–Heinemann, 2000.
[2] R. Butterfield, K. Bannerjee, *Boundary Element Methods in Engineering Science*, New York, 1981.
[3] C.A. Brebbia, *The Boundary Element Method for Engineers*, Pentech, London, 1984.
[4] R.H. Lyon, *Statistical Energy Analysis of Dynamical Systems*, Cambridge, MA, 1975.
[5] R.J.M. Craik, *Sound Transmission through Buildings using Statistical Energy Analysis*, Gower, England, 1996.
[6] K. De Langhe, *High-frequency Vibrations: Contributions to Experimental and Computational SEA Parameter Identification Techniques*, PhD Thesis, Katholieke Universiteit Leuven, Belgium, February 1996.
[7] L. Cremer, M. Heckl, *Structure Borne Sound: Structural Vibration and Sound Radiation at Audio Frequencies*, Springer, Berlin, 1973.
[8] J.C. Wohlever, R.J. Bernhard, Mechanical energy flow models of rods and beams, *Journal of Sound and Vibration* 153 (1) (1992) 1–19.
[9] O.M. Bouthier, R.J. Bernhard, Simple models of the energetics of transversely vibrating plates, *Journal of Sound and Vibration* 182 (1) (1995) 149–166.
[10] Y. Lase, M.N. Ichchou, L. Jezequel, Energy flow analysis of bars and beams: theoretical formulations, *Journal of Sound and Vibration* 192 (1) (1996) 281–305.
[11] B.R. Mace, P.J. Shorter, Energy flow models from finite element analysis, *Journal of Sound and Vibration* 233 (3) (2000) 369–389.
[12] R.S. Langley, On the vibrational conductivity approach to high frequency dynamics for two-dimensional structural components, *Journal of Sound and Vibration* 182 (4) (1995) 637–657.
[13] A. Carcaterra, A. Sestieri, Energy density equations and power flow in structures, *Journal of Sound and Vibration* 188 (2) (1995) 269–282.
[14] A. Le Bot, A vibro-acoustic model for high-frequency analysis, *Journal of Sound and Vibration* 211 (4) (1998) 537–554.
[15] L. Gagliardini, L. Houillon, L. Petrinelli, G. Borello, Virtual SEA: mid-frequency structure-borne noise modelling based on finite element analysis, *Proceedings of the SAE Noise and Vibration Conference*, Traverse City, Michigan USA, May 2003.
[16] E. Sadoulet-Reboul, A. Le Bot, J. Perret-Liaudet, M. Mori, H. Houjoh, A hybrid method for vibroacoustics based on the radiative energy transfer method, *Journal of Sound and Vibration* 303 (2007) 675–690.
[17] R.S. Langley, P. Bremner, A hybrid method for the vibration analysis of complex structural–acoustic systems, *Journal of Acoustical Society of America* 105 (3) (1999).
[18] P.J. Shorter, R.S. Langley, On the reciprocity relationship between direct field radiation and diffuse reverberant loading, *Journal of Acoustical Society of America* 288 (3) (2005) 669–699.
[19] P.J. Shorter, R.S. Langley, Vibro-acoustic analysis of complex systems, *Journal of Sound and Vibration* 117 (1) (2005) 85–95.
[20] C. Soize, A model and numerical method in the medium frequency range for vibroacoustic predictions using the theory of structural fuzzy, *Journal of the Acoustical Society of America* 94 (1993) 849–865.
[21] N. Vlahopoulos, X. Zhao, An investigation of power flow in the mid-frequency range for systems of co-linear beams based on a hybrid finite element formulation, *Journal of Sound and Vibration* 242 (3) (2001) 445–473.
[22] X. Zhao, N. Vlahopoulos, A basis hybrid finite element formulation for mid-frequency analysis of beams connected at an arbitrary angle, *Journal of Sound and Vibration* 269 (2004) 135–164.
[23] S.B. Hong, A. Wang, N. Vlahopoulos, A hybrid finite element formulation for a beam-plate system, *Journal of Sound and Vibration* 298 (1–2) (2006) 233–256.

[24] M. Viktorovitch, F. Thouverez, L. Jezequel, A new random boundary element formulation applied to high-frequency phenomena, *Journal of Sound and Vibration* 223 (2) (1999) 273–296.
[25] M. Viktorovitch, F. Thouverez, L. Jezequel, An integral formulation with random parameters adapted to the study of the vibrational behaviour of structures in the mid- and high-frequency field, *Journal of Sound and Vibration* 247 (3) (2001) 431–452.
[26] T.T. Soong, *Random Differential Equations in Science and Engineering*, Academic Press, New York, London, 1973.
[27] F.J. Fahy, A.D. Mohammed, A study of uncertainty in applications of sea to coupled beam and plate systems, part I: computational experiments, *Journal of Sound and Vibration* 158 (1) (1992) 45–67.